



HHS Public Access

Author manuscript

Pancreas. Author manuscript; available in PMC 2019 July 01.

Published in final edited form as:

Pancreas. 2018 July ; 47(6): 675–689. doi:10.1097/MPA.0000000000001075.

Advances in Diagnostic and Intraoperative Molecular Imaging of Pancreatic Cancer

Willemieke S. Tummers, MD,

Department of Radiology, Molecular Imaging Program at Stanford, Stanford University, Stanford, CA. Department of Surgery, Leiden University Medical Center, Leiden, The Netherlands

Juergen K. Willmann, MD,

Department of Radiology, Molecular Imaging Program at Stanford, Stanford University, Stanford, CA. Juergen K. Willmann died January 8, 2018

Bert A. Bonsing, MD, PhD,

Department of Surgery, Leiden University Medical Center, Leiden, The Netherlands

Alexander L. Vahrmeijer, MD, PhD,

Department of Surgery, Leiden University Medical Center, Leiden, The Netherlands

Sanjiv S. Gambhir, MD, PhD^{*}, and

Departments of Radiology, Bioengineering, and Materials Science & Engineering, Molecular Imaging Program at Stanford, Canary Center at Stanford for Cancer Early Detection, Stanford University, Stanford, CA

Rutger-Jan Swijnenburg, MD, PhD

Department of Surgery, Leiden University Medical Center, Albinusdreef 2, 2300 RC, Leiden, The Netherlands

Abstract

Pancreatic ductal adenocarcinoma (PDAC) has a dismal prognosis. In order to improve outcomes, there is a critical need for improved tools for detection, accurate staging and resectability assessment. This could improve patient stratification for the most optimal primary treatment modality. Molecular imaging, used in combination with tumor-specific imaging agents, can improve established imaging methods for PDAC. These novel, tumor-specific imaging agents developed to target specific biomarkers have the potential to specifically differentiate between malignant and benign diseases, such as pancreatitis. When these agents are coupled to various types of labels, this type of molecular imaging can provide integrated diagnostic, non-invasive imaging of PDAC as well as image-guided pancreatic surgery. This review provides a detailed overview of the current clinical imaging applications, upcoming molecular imaging strategies for PDAC, and potential targets for imaging, with an emphasis on intraoperative imaging applications.

Address correspondence to: R.J. Swijnenburg, Leiden University Medical Center, Albinusdreef 2, 2333 ZA Leiden, The Netherlands (r.j.swijnenburg@lumc.nl). Tel: +31 71 526 4005, Fax: +31 71 526 6750.

Conflict of Interest Disclosure: The authors declare no conflict of interest to the submitted work.

Disclosures

This manuscript describes the investigational use of Cetuximab-IRDye800, SGM-101, and [18F]FP-R01-MG-F2 not yet approved by the FDA.

Keywords

Molecular imaging; tumor-specific imaging; pancreatic cancer; intra-operative

INTRODUCTION

Pancreatic ductal adenocarcinoma (PDAC) accounts for about 90% of all pancreatic neoplasms and is the fourth most common cause of cancer-related deaths in developed countries.¹ PDAC has a dismal prognosis, with a five-year survival rate of less than 5%. Pain, jaundice and weight loss are the most common presenting symptoms but in the early stages of the disease, these symptoms may be subtle which often leads to delayed diagnoses.² The median size of PDAC at the time of diagnosis is ~3.1 cm, and these statistics have not changed in the past three decades despite advances in imaging technologies, as well as *in vitro* diagnostic testing methods.³ Resection of tumors while they are small, well-defined and localized results in a higher chance of complete tumor clearance which translates into greater patient survival rates.^{3,4}

Only 15% to 25% of patients are eligible for curative resection at their initial diagnosis, due to locoregional spread and metastasis.^{5,6} More precise detection methods can lead to improved patient stratification for the most optimal primary treatment modality; either surgery or systemic (neoadjuvant) therapy. This selection can prevent patients from undergoing resections without any oncologic benefit. Another advantage of precise visualization of the tumor could be a more radical resection. Tumor margin-positive (R1) resections occur in up to 70% of PDAC cases, leading to a high number of locoregional recurrence.^{7,8} This means that for all patients diagnosed with PDAC, only 15% of these patients will receive a radical, tumor-margin negative resection and have a chance for prolonged survival. Therefore, improved tools for diagnosis, accurate staging, and more effective, tumor-margin negative pancreatic surgeries are crucial for improving patient outcomes.⁹

Imaging techniques play an important role in the diagnosis of PDAC. Current clinical imaging protocols include transabdominal ultrasound, computed tomography (CT) and/or magnetic resonance imaging (MRI) for disease staging and prediction of resectability.¹ Endoscopic ultrasound (EUS) can complement these imaging methods with valuable staging information as well as the opportunity of tissue diagnosis by fine-needle aspiration.¹⁰

Molecular functional imaging has the potential to play an important role in PDAC management and be of complementary value to these conventional imaging techniques. It could be used for earlier tumor detection, and improved characterization, staging, and response assessment to neoadjuvant therapy. It could also serve as a guide for surgery during diagnostic laparoscopy and tumor resection. Possible imaging modalities for molecular imaging include molecularly-targeted contrast-enhanced transabdominal (CEUS) and EUS, CT, MRI, positron emission tomography (PET), photoacoustic imaging (PAI), fluorescence molecular imaging, and Raman optical imaging (Fig. 1).

Recently, Laeseke et al. published a review focused on the role of molecular imaging in early detection of PDAC.¹¹ The current review gives an overview of the status of clinical imaging applications, the advances of molecular imaging strategies, and most optimal imaging targets for PDAC, with a special emphasis on intraoperative applications.

CURRENT DIAGNOSTIC IMAGING TOOLS FOR PDAC

Transabdominal and endoscopic ultrasound

Ultrasound (US) is often the initial diagnostic assessment used in patients presenting with jaundice, weight loss, and abdominal pain. US is a relatively inexpensive, portable, noninvasive, and widely available tool. However, the sensitivity and accuracy of US is highly dependent on the operator's skills, degree of disease progression and body habitus of the patient. Therefore, sensitivity of conventional US for detecting PDAC varies widely and ranges from 95% in tumors > 3 cm to 50% in tumors < 1 cm.¹² In addition, it is difficult to differentiate between PDAC and inflammatory diseases such as pancreatitis using US technology.

EUS has become a valuable diagnostic tool for PDAC since it allows for tissue sampling and cytological evaluation, both of which can provide a definitive diagnosis.^{13,14} For the evaluation of solid pancreatic tumors, EUS detects lesions <2 cm with greater sensitivity (98%) than CT (86%). On the other hand, EUS also has important limitations in the evaluation of solid pancreatic lesions. First, there is substantial operator-dependence, resulting in variable sensitivity ranging from 57% to 81%.^{15,16} Second, the sensitivity is relatively poor (80%) when detecting PDAC in patients with pancreatitis.¹⁷ And finally, the invasive nature of EUS is a significant disadvantage of this technique.

Computed Tomography

Multiphase multi-detector row CT (MDCT) with intravenous contrast is the diagnostic test of choice for suspected pancreatic lesions. MDCT has the highest accuracy in determining the extent of primary tumor, locoregional extension, vascular invasion, distant metastases and resectability.¹⁴ MDCT is used to predict resectability of PDAC with a positive predictive value (PPV), sensitivity and specificity of 89%, 96% and 33–72%, respectively.^{18,19} An additional advantage of MDCT imaging is the possibility to detect extrapancreatic spread by perineural invasion.²⁰ This is of great importance since these patients have significantly reduced survival after pancreaticoduodenectomy.²¹ CT perfusion can be used to differentiate between low and high grade PDAC, by using peak enhancement intensity values and blood volume parameters.²² Despite its sensitivity, MDCT cannot reliably detect small lesions (<1cm), differentiate between malignant lesions and benign conditions, or detect isoattenuating primary tumors.²³

Magnetic Resonance Imaging

MRI has a reported sensitivity and specificity for diagnosis of PDAC of 85–93% and 72–79%, respectively.^{24,25} MRI has advantages over CT regarding improved soft tissue contrast resolution and the absence of ionizing radiation. This leads to several situations where MRI is preferred above CT; such as with small tumors, isoattenuating lesions, and fatty infiltration

in the pancreatic head.²⁶ In addition, there are alternative sequences when using MRI, such as magnetic resonance cholangiopancreatography (MRCP) which can be used to image the biliary and pancreatic ducts in detail. MRCP has comparable sensitivity to the more invasive endoscopic retrograde cholangiopancreatography (ERCP) in diagnosing PDAC.²⁷ Another potential sequence is diffusion-weighted images (DWI), with this technique the difference in diffusion of water molecules is visualized by using the apparent diffusion coefficient (ADC). PDAC tends to have low ADC values due to high levels of fibrosis. This methods is helpful for the identification of subtle lesions with diffusion restriction.²⁶ Due to its high soft tissue contrast MRI is the preferred modality for assessing cystic lesions in the pancreas.²⁸ Another important advantage of MRI over CT is the more precise detection of enlarged lymph nodes and distant metastases.²⁸ A disadvantage of both CT and MRI, is that neither can reliably distinguish residual or necrotic tumor from fibrosis and radiation changes after treatment.

PET Imaging

Currently, PET is the only molecular imaging technique used for PDAC. It enables whole body imaging to allow staging of diseases, similar to CT and MRI. [¹⁸F]-2-fluoro-2-deoxyglucose (¹⁸F-FDG)-PET has an established role in the work-up of various malignancies. The normal pancreas has low glucose usage compared to PDAC, so areas with increased uptake can be visualized and point towards potential lesions. Because the metabolic activity of a tumor is expressed by the degree of ¹⁸F-FDG uptake it is possible to predict tumor aggressiveness and even survival in patients by the degree of uptake.^{29,30} The average sensitivity and specificity of ¹⁸F-FDG for PDAC are 94% and 90% respectively, compared to 82% and 75% for CT.³¹ Choi et al. reported the use of ¹⁸F-FDG-PET to detect biologically active tumor volumes and therefore to assess treatment effectiveness.³² A recent multi-center trial in the UK with 550 patients looking at the diagnosis of PDAC showed a sensitivity of 92.7% for FDG PET/CT compared to 88.5% for MDCT ($P = 0.010$) and a specificity of 75.8% compared to 70.6% ($P = 0.023$).³³ A problem of using ¹⁸F-FDG uptake, is that glucose metabolism is not specific for malignant processes, and physiologic uptake can be found in normal tissues as well as in inflammatory tissue which might lead to false-positive findings, causing a similar appearance for pancreatitis and PDAC.³⁴

CURRENT INTRA-OPERATIVE IMAGING TOOLS

A major limitation of the aforementioned imaging techniques, such as CT, MRI or PET is the fact that these techniques cannot be applied as intraoperative imaging tools due to altered positioning of the body, and tissue manipulation by the surgeon.³⁵ For brain cancer surgery, the use of MRI-guided resection has almost become standard practice.³⁶ Unfortunately, this method is time-consuming, costly. Therefore, chances are low that MRI-guided resection will be widely-implemented outside the field of brain cancer surgery. Currently, the only tools available for a pancreatic surgeon to ensure complete tumor resection are visual and tactile information, frozen-section analysis by a pathologist, and intra-operative ultrasound.

Intra-operative frozen-section analysis (IFSA) is commonly performed to determine resectability when unanticipated locoregional spread is identified during surgery and to

ensure negative final margins after resection.³⁷ Although frozen section analysis is commonly used to determine successful ablation, it is time-consuming, and only samples a small fraction of the wound bed which could lead to false-negative results. During surgery, if the IFSA of the resection margin turns out to be positive, additional pancreatic tissue is often removed in an effort to clear the margin. Only a few single institutional studies have assessed the value of this surgical maneuver so far and it is shown that there is actually no improved overall survival when additional IFSA-guided resection is performed.^{38–40} IFSA has a reported low incidence of false-positive results, but the amount of false-negative results has ranged widely from 1.2% to 75%.^{41,42} This relatively high incidence of false-negative results could indicate that preoperative imaging and possibly even surgical judgement are more reliable than a negative IFSA.

Intra-operative Ultrasound

Currently, the only intra-operative imaging technique to help the surgeon delineate PDAC from its surrounding structures is anatomical intraoperative ultrasound. The ability to provide high resolution real-time imaging, along with accurate lesion detection, has established the role of intraoperative ultrasound (IOUS) in PDAC surgery. IOUS can be used for intraoperative guidance and localization of lesions, for determining resectability, surgical planning, differentiation between cystic and non-cystic lesions, and metastatic survey.^{43,44} IOUS also has disadvantages since it is less reliable for detecting superficial and small lesions compared to visual and tactile methods.⁴⁵ Another disadvantage is its operator dependence; substantial training and experience are essential for generating and interpreting useful images for intra-operative surgical decision-making.^{12,46}

THE NEED FOR ADVANCED MOLECULAR IMAGING IN PDAC

To be able to improve detection and patient stratification for treatment, there is a critical need to develop and improve imaging methods that specifically recognize cancer.⁴⁷ In current practice, the accurate identification of tumors is mainly subjective and relies heavily on the surgeon's experience leading to a significant variability in surgical outcomes.⁴⁸ This inability to exactly identify tumors intraoperatively could result in: 1) Incomplete resection of tumors that could otherwise have been resected completely; 2) Attempt to resect tumors which should have been identified as locally advanced tumors; 3) Incomplete lymph node clearance due to lack of knowledge of the involved or potentially involved lymph nodes, and 4) Resection of the primary tumor in the presence of visually occult micrometastasis. In each of these situations, patients undergo operations with little or no oncological benefit, but with a high risk of deterioration of quality of life due to surgery in their end stage of life. There are two other challenges a surgeon faces when resecting PDAC. First, both the benign pancreatitis and malignant PDAC have abundant stroma, and therefore both entities are difficult to distinguish using conventional imaging techniques. Second, the introduction of neoadjuvant treatment regimens such as FOLFIRINOX, leading to a 51% increase in tumors becoming resectable after 4 months of neoadjuvant treatment.⁴⁹ One of the major drawbacks after neoadjuvant treatment is that conventional imaging modalities, such as CT and MRI, are often not able to differentiate between viable tumor and chemoradiation-induced tumor necrosis and fibrosis, and, therefore, prediction of resectability is limited.⁵⁰ Neoadjuvant

treatment effects make differentiation between (vital) tumor and fibrotic pancreatic tissue even harder for surgeons during the operation.

Tumor-targeted molecular imaging could provide crucial information in these situations. Molecular imaging can either be performed by using conventional imaging techniques in combination with tumor-specific imaging agents, or by the development of novel imaging techniques, such as fluorescent, photoacoustic and Raman optical imaging. Currently, several first-in-human clinical trials are conducted using these techniques in pancreatic cancer patients.

TUMOR-TARGETED MOLECULAR IMAGING STRATEGIES FOR PDAC

A molecular imaging approach using imaging agents that target molecular features of cancer could lead to more precise diagnoses.¹³ The common consensus is that PDAC evolves from precursor lesions that transform into invasive carcinoma through a multistep process, that involves the progression from pancreatic intraepithelial neoplasia (PanIN) into PDAC.⁵¹ Genetic alterations, such as mutations in the KRAS oncogene or p53, DPC4, and BRCA2 tumor suppressor genes affect a core group of signaling pathways. The processes that are altered in PDAC lead to the expression of specific biomarkers, and these changed biomarkers may serve as targets for tumor-specific imaging.⁵² Potential biomarkers for tumor-specific targeting must possess certain characteristics such as diffuse upregulation through tumor tissue, strong upregulation compared to the expression in normal and surrounding tissue, and localization on the cellular membrane.^{53, 54} An effective molecular imaging agent needs to demonstrate a high ratio of specific to non-specific binding to make sure the signal truly reflects the molecular imaging target.

There are numerous categories of available molecular imaging agents including small molecules, peptides, aptamers, antibodies, engineered protein fragments, nanoparticles, or micro-sized contrast agent. Each of these types of agents is different in size and thus possesses different pharmacokinetic characteristics (Table 1). It goes beyond the scope of this review to describe all the different molecular imaging agents in detail; however, please refer to the following review for further details.⁵⁵

The most important groups of targeted imaging agents that are currently being explored are based on targeting specific receptors that are upregulated during the progress of PDAC development. For example, global expression analysis of PDAC has revealed that claudin 4 and prostate stem cell antigen (PSCA) are upregulated in the vast majority of PDACs.^{56,57} Given the membrane localization and the presence of an extracellular domain, these proteins are attractive candidates for targeted imaging. Additionally, claudin 4 has a high expression in high grade PanIN lesions, indicating the potential to detect lesions before development into an invasive carcinoma.⁵⁸ Other targets employed for tumor-specific imaging of different cancer types are not applicable for PDAC due to co-expression of these receptors on normal pancreatic tissue (somatostatin, secretin, bombesin, cholecystokinin, vasoactive intestinal peptide).^{59–62} Another possibility for PDAC would be the use of a combined target, against both tumor and surrounding stroma, which can be of significant advantage because of the abundance of stroma in PDAC, such as the target uPAR.⁶³ Since several potential imaging

targets have been identified for normal pancreatic tissue, an alternative strategy could be to visualize normal tissue while abnormal/cancerous would be visualized by a lack of imaging signal. For example by targeting the bombesin receptor, PDAC would appear by a lack of contrast agent uptake.⁶⁴ However, specificity of those potential molecular imaging targets compared to pancreatitis is still to be determined.

MOLECULARLY TARGETED IMAGING AGENTS FOR CURRENT CLINICAL IMAGING MODALITIES

Molecularly Targeted (Intra-operative) Ultrasound

Contrast-enhanced US (CEUS) involves the use of targeted microbubble imaging agents and specialized imaging techniques. For the diagnosis and differentiation of pancreatic malignancies, transabdominal CEUS has generated test characteristics comparable to, or better than other diagnostic modalities such as conventional ultrasound and CT.⁶⁵ CEUS with a non-specific agent showed similar sensitivity to contrast-enhanced CT for the detection of PDAC (91.7% and 97.2%, respectively) and of pancreatitis (82.1% and 67.9%, respectively).⁶⁶ Intra-operative CEUS is well established in liver surgery, but it has not yet found its place in PDAC. However, CEUS provides a potential for the detection of small tumors, since it shows improved sensitivity and specificity compared to multi-detector CT (MDCT) for pancreatic lesions <2 cm; 91% vs 71% and 94% vs 92%, respectively.⁶⁷

Ultrasound using molecularly targeted microbubbles would be a tool to increase sensitivity and specificity even further.⁶⁸ Targeted imaging agents differ from those initially developed by the presence of a targeting moiety able to link the microbubble to the selected biomarker.^{68–72} A disadvantage of microbubbles is their relatively large diameter. Therefore, they remain within the vascular compartment after intravascular administration, which limits targeting to molecules that are overexpressed on the surface of endothelial cells of the tumor vasculature (Fig. 2).⁷³

Molecular-targeted Agents for Ultrasound Imaging—The formation of new blood vessels is a fundamental process during tumor progression. Under hypoxic conditions, which are required for effective tumor angiogenesis, expression of hypoxia-inducible factors is induced in endothelial vessels resulting in vascular endothelial growth factor receptor (VEGFR) expression.⁷⁴ VEGFR is a receptor tyrosine kinase that mediates most of the proangiogenic activity of VEGF. Our group has previously shown that VEGFR2 is a promising target for detection of PDAC. In a cohort of 129 patients, VEGFR2 was abundantly expressed in up to 72% of all PDAC cases.⁷⁵ Microbubbles developed to recognize VEGFR2, integrin and endoglin were used to visualize tumor angiogenesis by ultrasound imaging in PDAC of genetically engineered mouse models.^{76,77} Recently, first-in-human clinical trials using a VEGFR2-targeted agent have been performed.⁷² and shown great potential in detecting breast and ovarian cancer.⁷⁸ Foygel et al discovered and validated thymocyte antigen 1 (Thy1) as a new PDAC imaging target.⁷⁹ Thy1 is a marker expressed on the neovasculature of PDAC and shown to be differentially expressed in PDAC versus pancreatitis and normal pancreatic tissue in humans.⁷⁹ In vivo imaging studies with a genetically engineered mouse model of PDAC showed a 4–5.5-fold increased signal in

PDAC compared to normal parenchyma when using a novel Thy1-targeted microbubble.⁷⁹ Clinical trials with these agents in PDAC patients have not yet been performed, but are planned for the future.

Molecularly Targeted MRI

MRI has a fairly high sensitivity as described above, but increased sensitivity could be realized by increased enhancement of the tumors using molecularly-targeted contrast agents. Pirolo et al described a way to systemically deliver the imaging agent gadolinium in a tumor-targeted nanocomplex leading to better tissue penetration, and therefore better visualization of PDAC in an orthotopic animal model.⁸⁰

Molecular-targeted Agents for MRI—Studies using targeted MR imaging against biomarkers, such as plectin-1 and EGFR, showed tumor targeting both ex vivo and in vivo.^{81,82} ScFvEGFR-IO injection lead to 4.8 fold specific decrease in MRI signal in the tumor area, compared to a non-targeted particle.⁸¹ Mucin-1 is a tumor-specific antigen that is one of the early hallmarks of carcinogenesis in a broad range of tumors, including PDAC.⁸³ Medarova et al. developed a dual-modality imaging agent targeting Mucin-1 in an orthotopic PDAC model for both MRI and NIRF imaging.^{83,84} A potential drawback for clinical use of mucin-1 as imaging target is that this antigen expression is down-regulated after neoadjuvant gemcitabine therapy.⁸⁵

Molecularly Targeted PET

The specificity of PET imaging could be improved by using a more disease-specific imaging agent compared to FDG-PET (Fig. 3). There are several preclinical examples of disease-specific PET imaging in PDAC, and recently, for the first time a first-in-human trial is performed by Kimura et al. using a tumor-specific peptide targeting integrin $\alpha v \beta 6$, [18F]FP-R01-MG-F2, for the detection of PDAC. This study shows proof even in this cancer type with dense stroma, an imaging agent can penetrate the tumor [Kimura et al under review].

Molecularly Targeted Agents for PET Imaging—In preclinical setting, several targets are explored. Aung et al described the use of ⁶⁴Cu-RAFT-RGD, targeting $\alpha v \beta 3$, for imaging an orthotopic pancreatic tumor-bearing mouse model showing higher detectability of cancer cells as compared to ¹⁸F-FDG-PET.⁸⁶ Carbohydrate antigen 19-9 (CA 19-9) is widely used as a serum marker of PDAC, and it is known to be presented on the tumor cells of approximately 90% of all PDAC patients.^{87, 88} A dual-modal probe targeting CA 19-9 using PET and near-infrared fluorescence imaging was developed by Houghton et al. This probe identified metastases and map sentinel lymph nodes in an orthotopic PDAC mouse model via both PET-computed tomography (PET/CT) and NIRF imaging.⁸⁹ Unfortunately, CA 19-9 is also presented on pancreatitis and therefore, this agent will be of limited value in the clinic.⁹⁰ The earlier mentioned cell surface receptor integrin $\alpha v \beta 6$ is a well-known target for molecular imaging of PDAC since over 90% of human PDAC cases overexpress $\alpha v \beta 6$.^{91–96} Hackel et al. used two version of an ¹⁸F-labeled integrin $\alpha v \beta 6$ -targeted cystine knot peptide for successful PET-imaging of PDAC xenografted tumors in mice.⁹¹ Tissue factor (TF), a transmembrane glycoprotein, is also known to be upregulated during tumor growth and metastasis. There is a strong correlation between the aberrant expression of TF, staging and

overall survival in PDAC, making TF an attractive imaging target.^{97, 98} Hong et al. developed a PET tracer, ⁶⁴Cu-NOTA-ALT-836, for imaging TF expression using the chimeric antihuman TF monoclonal antibody, ALT-836. Serial PET revealed that the uptake of (⁶⁴Cu)-NOTA-ALT-836 was significantly higher in TF positive tumors compared to negative tumors.⁹⁹ Activated leukocyte cell adhesion molecule (ALCAM) homotypic interactions promote primary tumor growth, and this cell-surface glycoprotein is upregulated on cancer cells relative to normal cells.¹⁰⁰ McCabe et al. imaged ALCAM expression by using a cysteine-modified diabody, CysDb, which binds specifically to ALCAM-positive cells with a binding affinity of 1–3 nM and microPET images showed specific targeting of positive tumors.¹⁰¹ Clinical translation of this probe seems unlikely due to its relatively short half-life and potential nephrotoxicity due to high renal exposure of the beta-emitting radionuclide. Alternatively, this agent could be labeled with ¹⁸F, which would overcome these limitations. Lastly, the transferrin receptor (TfR) was investigated as a possible target for PET imaging in PDAC. TfR is a cell-surface receptor involved in iron uptake. It is overexpressed on cells with high proliferation rates, and about 80% of all PDAC patients show high TfR expression.¹⁰² Sugyo et al. developed a PET probe targeting TfR, with a mean tumor-to-muscle ratio of 9.8 at day 6 in a subcutaneous PDAC model. However, a major disadvantage of this probe is its high accumulation in the liver, which could hinder detection of tumor tissue in close proximity to the liver.¹⁰³

INTRAOPERATIVE MOLECULAR IMAGING TECHNIQUES: POTENTIAL FOR IMPROVED INTRA-OPERATIVE PERFORMANCE

Fluorescence Molecular Imaging

Over the last few years, intraoperative imaging technologies using near-infrared (NIR) fluorescence have made enormous progress. The volume of publications in this field has increased eightfold in the literature in the last 10 years.¹⁰⁴ Benefits of Fluorescence imaging using NIR fluorescent light include the ability to image in real time using an NIR fluorescence camera system without impeding the current clinical workflow. If surgeons were able to resect tumors and preserve normal structures more easily, time of surgery could be shortened, thereby reducing anesthesia time and its associated risks. Furthermore, this could subsequently lower rates of recurrence and complications, which would improve patient outcomes and even drive down costs.³⁵ Fluorescence imaging using NIR fluorescent light has already been established as a powerful tool for guiding precise intra-operative positioning in other types of cancer such as liver metastases,¹⁰⁵ breast cancer,^{106,107} ovarian cancer,¹⁰⁸ melanoma,¹⁰⁹ vulvar cancer,^{110,111} and cervical cancer.^{112,113} Currently, only the non-specific dyes methylene blue (MB) and indocyanine green (ICG) are approved for clinical use by the FDA and in order to determine the true clinical benefit of tumor-specific fluorescent imaging, developing and clinically assessing tumor-specific imaging agents will be essential (Fig. 4). Recently, two first-in-human clinical studies are performed by our research groups using tumor-specific intra-operative imaging in PDAC, targeting CEA with SGM-101 [Hoogstins et al under review] and EGFR with cetuximab-IRDye800 [Tummers WS et al. accepted]. Hoogstins et al performed a phase 1 clinical trial targeting CEA, with a 700nm fluorescent agent [Hoogstins et al under review]. Tummers et al conducted a clinical trial using both NIR and PA imaging for the tumor-specific detection of PDAC with

cetuximab-IRDye800 [Tummers et al accepted]. In both trials successful PDAC imaging could be performed, however interfering autofluorescence was seen with the fluorescent agent at 700 nm. These trials show the first proof that this imaging technique is possible in PDAC, despite the idea that the dense stroma of PDAC will restrict targeted-imaging and therapy. Tummers et al. even show proof of drug penetration into the a single tumor duct.

Molecular-targeted Agents for Fluorescent Molecular Imaging—As described above, until now only agents targeting the CEA and EGFR receptor are used in clinical trials for NIR fluorescent imaging of PDAC. With cetuximab-IRDye800, it was even possible to establish a significantly different fluorescent signal in PDAC compared to peritumoral inflammation [Tummers et al accepted]. Furthermore, only preclinical work is performed for the identification of intraoperative imaging agents and targets. As mentioned before, $\alpha v \beta 6$ seems to be a reliable target for PDAC. Gao et al. synthesized an integrin $\alpha v \beta 6$ -targeted near-infrared phthalocyanine dye-labeled agent, termed Dye-SA-B-HK, and investigated it for possible targeted theranostics. Dye-SA-B-HK specifically bound to integrin $\alpha v \beta 6$ in vitro and in vivo with high receptor binding affinity, and when used for surgical guidance, the tumors were successfully removed completely.⁹³ The main advantage of this agent compared to nanoparticles is the size of this agent, which gives the ability to extravasate, and faster excretion. Zhang et al. recently developed an optical imaging agent, suitable for both fluorescent and photoacoustic imaging. This imaging agents consists of a cysteine knottin targeting $\alpha v \beta 6$ conjugated to the dye Atto-740, A740-R01. The agent was able to successfully detect integrin $\alpha v \beta 6$ both in vitro and in vivo by photoacoustic and fluorescence imaging.¹¹⁴

Cathepsin E (Cath E) is a tumor-associated intracellular non-lysosomal aspartic proteolytic enzyme. In normal physiology Cath E is expressed in immune cells. In the pancreas, Cath E is present in PanIN lesions and PDAC, but not in normal pancreatic tissue.¹¹⁵ Targeting Cath E can be done by Cath E-activatable imaging probes. These agents are nonfluorescent or produce low-fluorescence in their unactivated state, but become fluorescent after activation as a result of binding to their molecular target such as a tumor-specific enzyme.^{35,115,116} Using an activatable imaging probe has several advantages. First, in its native state the quenched probe is optically silent, thereby minimizing background fluorescence and enhancing tumor-to-background ratios. Second, protease recognition sites allow for specific activation of probes. Finally, probes can be designed to be activated by different proteases, thus permitting specific detection of tumors with different protease expression profiles.^{117,118} Recently, Whitley et al. published results of the first-in-human trial using a protease-activated fluorescent imaging probe, LUM015, to detect soft tissue sarcoma or breast cancer. This study demonstrated the probe's safety in humans and also its tumor-specific fluorescence.¹¹⁹

Despite improved tissue penetration as compared to visible light, an essential limitation of the use of NIR fluorescence imaging intraoperatively is its inability to visualize structures deeper than approximately 5 – 8 mm below the surface.^{35,120} As a result of this limitation, the field has been shifting towards developing a combination of different forms of imaging modalities, such as PAI, as described in the clinical trial of Tummers et al.

Photoacoustic Imaging

Photoacoustic imaging (PAI), also referred to as optoacoustic imaging, is a relatively new imaging technique with significant promise. PAI provides real-time, noninvasive imaging of the optical absorption properties of tissues. PAI relies on the photoacoustic effect; a pulsed nanosecond-long red-shifted laser beam that is used to stimulate localized thermoplastic expansion of the tissues. This expansion generates pressure waves, synonymous with those produced in ultrasound, which can be detected by a transducer and converted into images.¹²⁰ The combined use of light and sound gives PAI an important advantage over other imaging modalities including CT, PET or ultrasound because it provides unique scalability of its spatial resolution. The penetration up to clinically relevant depths, namely from 6 mm to 5 cm, is an important factor for its potential intraoperative use during PDAC surgery (Fig. 5).^{120–123}

PAI can be performed based on two methods: by relying on the differences in the optical absorption properties of endogenous tissue or by using exogenous imaging agents targeting a specific molecular process of interest. Exogenous imaging agents have the ability to greatly enhance the contrast generated by PAI. The selection of an imaging agent will depend on the application for which it will be used. Design considerations and requirements for a PAI imaging agent include: (1) ease of synthesis, (2) overall size on the nano-scale or smaller in order to extravasate the vascular compartment, (3) a large absorption cross-section of light in the NIR wavelength region where light penetration into tissue is maximized, (4) a surface chemistry that allows simple bioconjugation of targeting moieties, (5) proven safety profile, and (6) a structural and molecular biostability in biological fluids.¹²⁴ Photostability is also very important for these agents as they often suffer from loss of optical absorption (photobleaching) due to exposure to prolonged pulsed laser irradiation.¹²⁵ Nanoparticles are the most commonly used types PAI agents, and especially gold nanoparticles, single-walled carbon nanotubes (SWNT), and quantum dots.^{120,124,126,127} Gold nanoparticles have an advantage in that their optical properties are highly tunable over the NIR spectrum by varying their size and shape. However, they have major disadvantages since they consist of gold, which is not approved for human use, and they can become deformed after extended exposure to laser radiation.¹²⁸ SWNTs absorb light over a broad spectrum, and targeting agents can easily be conjugated for molecular imaging. Quantum dots are strongly fluorescent and have been shown in multiple studies to be successful PAI agents in PDAC.^{129,130} Other important disadvantages of gold nanoparticles, SWNTs, and quantum dots are their inability to sufficiently extravasate and the potential long term effects due to retention in the reticuloendothelial system which are not an issue for small particles.^{131,132}

As previously stated, the strengths of PAI include its clinically relevant depth penetration compared to fluorescence imaging and the potential to visualize extravascular molecular imaging targeted compared to molecular CEUS. The main disadvantages of PAI are its inability to image through bone or air-filled structures, and the fact that no commercial intraoperative systems are available for now.⁵⁵ Clinical applications for molecular photoacoustic imaging are still being explored. For diagnostics in PDAC, PAI could potentially be used during EUS in order to improve the sensitivity of the procedure. Studies investigating the intraoperative use of PAI are limited, and only described by Tummers et al. By targeting the

EGFR receptor, a significant difference was shown in PA signal in the tumor and surrounding pancreatic tissue. This indicates that intraoperatively PAI could potentially help determining the extent of the tumor infiltration before removal, tumor delineation, and the completeness of removal following resection and also play an important role in the assessment of metastases and lymph node status.¹²⁰

Molecular-targeted Agents for Photoacoustic Molecular Imaging—In preclinical studies, the first use of targeted photoacoustic imaging using SWNT was described by De La Zerda et al. in 2008. Intravenous administration of SWNT conjugated to cyclic Arg-Gly-Asp (RGD) peptides in mice bearing tumors showed eight times greater photoacoustic signal compared to mice injected with non-targeted nanotubes.¹²⁷ Levi et al. developed and validated both tumor-specific PAI agents for prostate cancer, against gastrin-releasing peptide receptor,¹³³ and for follicular thyroid carcinoma, against MMP-9.¹³⁴ Both agents showed increased PAI signal compared to a control agent. Conjugated polymers (CPs) are upcoming optical imaging agents that have unique chemical and optical properties thus allowing them to be used as imaging agents for PAI among other technologies.¹³⁵ Balasundaram et al. used folate-CP dots for the molecular imaging of breast cancer and showed a strong PA signal compared to non-specific CP dots.¹³⁶ Promising PAI agents are activatable agents, as firstly described by Levi et al. targeting a proteolytic enzyme, e.g. MMP-2, which is photoacoustically silent before cleavage and leads to PAI signal after activation by the target.¹³⁷

To tackle the abovementioned limitation fluorescence guided surgery is facing with limited depth penetration, PAI could help determining the extent of tumor before removal, and the completeness of the resection intraoperatively. On the other hand, fluorescent imaging has a superior sensitivity for superficial lesions. By combining the two modalities, the strengths of both NIR fluorescence imaging and PAI have the potential to overcome the limitations of the individual techniques in a combinatorial fashion.

Raman Optical Imaging

Raman optical imaging is based on the Raman effect, a process discovered by Chandrasekhara Venkata Raman in 1928 that is based on the inelastic scattering of light. Objects made of different molecular compositions will scatter light differently and produce unique spectra that are a function of the chemical bonds contained in the molecule of interest. Unfortunately, Raman scatter is very weak, with less than one in a million incident photons experiencing this effect.^{120,138,139} When the scattering molecule is placed on a surface of a roughened plasmonic substrate, the signal is increased by many log orders and is known as surface-enhanced Raman scattering (SERS).^{140,141} A major advantage of Raman optical imaging is the potential to detect multiple SERS nanoparticles simultaneously (a process called multiplexing), by modifying the Raman active layer that is absorbed onto the metal surface.¹³⁸ Raman spectroscopy is recently tested *ex vivo* on human colon tissue. Zavaleta et al developed a Raman spectroscope in combination with a multiplexed panel of tumor-targeting Raman nanoparticles, to rapidly distinguish between normal and precancerous tissues and to identify flat lesions in the colon.¹⁴² This technology could be used for helping endoscopists or surgeons to delineate tumors while performing procedures.

^{143,144} Additionally, Jermyn et al. developed a handheld contact Raman spectroscopy probe for the detection of cancer cells in the human brain. Intra-operatively, they were able to differentiate normal brain from cancer and normal brain invaded by cancer with a cellular resolution with sensitivity of 93% and specificity of 91% in humans.¹⁴⁵ Kircher et al described a MRI-PAI-Raman imaging nanoparticle to delineate the margins of brain tumors. This triple-modality-nanoparticle approach combines the strengths of the three modalities and leads to more accurate brain tumor imaging and resection in mouse models.¹⁴⁶ A variation on Raman spectroscopy, transmission Raman spectroscopy, has enabled identification of calcifications at depths of up to 2.7 cm in breast tissue.¹⁴⁷ This technique could potentially be used in the differentiation between PDAC and pancreatitis, since the latter is known for containing abundant calcifications. However, continued development of Raman spectroscopic instrumentation is needed in order to perform at the level necessary for intraoperative clinical use, including the design of a probe and the complete hardware which will need to be compact and easily integrated into the clinical OR.¹⁴⁸

SUMMARY AND CHALLENGES FOR THE FUTURE

Despite great efforts to improve treatment for patients with PDAC in recent years, the disease still has the worst prognosis of all major solid cancers. Molecular imaging using tumor-targeting agents and various modalities has shown great potential, both clinically and preclinically, in order to bridge the gap between diagnostic and intraoperative imaging for PDAC treatment, and for monitoring response to perioperative chemo- and or radiotherapy. Multimodal imaging modalities also have significant potential when used as an integrated diagnostic and intraoperative technology, since this can overcome limitations of the individual modalities. At this point, feasibility of tumor-specific PET and fluorescence is shown in PDAC patients, and as soon as the other modalities are translated into the clinic the full potential of tumor-specific molecular can be assessed (Fig. 6).

The discovery of the perfect target (Table 2) and translation of molecular-targeted imaging to the clinic remains challenging due to the need for specific exogenous imaging agents in order to image the biochemical process of interest. The discovery and validation of such imaging targets is time-consuming and expensive, and rarely results in a clinically useful agent. Many of the imaging probes reported in animal models have failed to reach the clinic and are still in the investigational stage. Unfortunately, the extensive approval process of the FDA makes it impossible to quickly test imaging probes in a clinical pilot study in order to determine effectiveness in humans and thus save resources and concentrate on more promising probes.¹⁴⁹ In addition, the added value of molecularly-targeted imaging to patient benefit still needs to be proven before wide-spread use of this technique is expected. This needs to be accomplished by increasing the number of human trials using a standardized technique to demonstrate safety and effectiveness. Although this is still far from current reality, the bulk of preclinical studies and the first successful clinical studies outlined in this review, show that more wide-spread clinical use is on the horizon.

Acknowledgments

Financial support: This work was supported in part by NIH R21EB022770 (JKW), and NIH R41CA203090 (JWK). Willemieke S Tummers contribution to this work was supported in part by Michaël-van Vloten Fonds.

References

1. Vincent A, Herman J, Schulick R, et al. Pancreatic cancer. *Lancet*. 2011; 378:607–620. [PubMed: 21620466]
2. Jang JY, Kang MJ, Heo JS, et al. A prospective randomized controlled study comparing outcomes of standard resection and extended resection, including dissection of the nerve plexus and various lymph nodes, in patients with pancreatic head cancer. *Ann Surg*. 2014; 259:656–664. [PubMed: 24368638]
3. Tummala P, Junaidi O, Agarwal B. Imaging of pancreatic cancer: An overview. *J Gastrointest Oncol*. 2011; 2:168–174. [PubMed: 22811847]
4. Agarwal B, Correa AM, Ho L. Survival in pancreatic carcinoma based on tumor size. *Pancreas*. 2008; 36:e15–20.
5. Stathis A, Moore MJ. Advanced pancreatic carcinoma: current treatment and future challenges. *Nat Rev Clin Oncol*. 2010; 7:163–172. [PubMed: 20101258]
6. Barugola G, Partelli S, Marcucci S, et al. Resectable pancreatic cancer: who really benefits from resection? *Ann Surg Oncol*. 2009; 16:3316–3322. [PubMed: 19707831]
7. Verbeke CS. Resection margins and R1 rates in pancreatic cancer--are we there yet? *Histopathology*. 2008; 52:787–796. [PubMed: 18081813]
8. Verbeke CS, Leitch D, Menon KV, et al. Redefining the R1 resection in pancreatic cancer. *Br J Surg*. 2006; 93:1232–1237. [PubMed: 16804874]
9. Gao D, Gao L, Zhang C, et al. A near-infrared phthalocyanine dye-labeled agent for integrin alphavbeta6-targeted theranostics of pancreatic cancer. *Biomaterials*. 2015; 53:229–238. [PubMed: 25890722]
10. Hartwig W, Werner J, Jager D, et al. Improvement of surgical results for pancreatic cancer. *Lancet Oncol*. 2013; 14:e476–e485. [PubMed: 24079875]
11. Laeseke PF, Chen R, Jeffrey RB, et al. Combining in Vitro Diagnostics with in Vivo Imaging for Earlier Detection of Pancreatic Ductal Adenocarcinoma: Challenges and Solutions. *Radiology*. 2015; 277:644–661. [PubMed: 26599925]
12. Balci NC, Semelka RC. Radiologic diagnosis and staging of pancreatic ductal adenocarcinoma. *Eur J Radiol*. 2001; 38:105–112. [PubMed: 11335092]
13. Cote GA, Smith J, Sherman S, et al. Technologies for imaging the normal and diseased pancreas. *Gastroenterology*. 2013; 144:1262–1271. [PubMed: 23622136]
14. Kramer-Marek G, Gore J, Korc M. Molecular imaging in pancreatic cancer--a roadmap for therapeutic decisions. *Cancer Lett*. 2013; 341:132–138. [PubMed: 23941833]
15. Haycox A, Lombard M, Neoptolemos J, et al. Review article: current practice and future perspectives in detection and diagnosis of pancreatic cancer. *Aliment Pharmacol Ther*. 1998; 12:937–948. [PubMed: 9798798]
16. Ahmad NA, Kochman ML, Brensinger C, et al. Interobserver agreement among endosonographers for the diagnosis of neoplastic versus non-neoplastic pancreatic cystic lesions. *Gastrointest Endosc*. 2003; 58:59–64. [PubMed: 12838222]
17. DeWitt J, Devereaux B, Chriswell M, et al. Comparison of endoscopic ultrasonography and multidetector computed tomography for detecting and staging pancreatic cancer. *Ann Intern Med*. 2004; 141:753–763. [PubMed: 15545675]
18. Ellsmere J, Morteale K, Sahani D, et al. Does multidetector-row CT eliminate the role of diagnostic laparoscopy in assessing the resectability of pancreatic head adenocarcinoma? *Surg Endosc*. 2005; 19:369–373. [PubMed: 15624058]
19. Zamboni GA, Kruskal JB, Vollmer CM, et al. Pancreatic adenocarcinoma: value of multidetector CT angiography in preoperative evaluation. *Radiology*. 2007; 245:770–778. [PubMed: 17951353]
20. Deshmukh SD, Willmann JK, Jeffrey RB. Pathways of extrapancreatic perineural invasion by pancreatic adenocarcinoma: evaluation with 3D volume-rendered MDCT imaging. *AJR Am J Roentgenol*. 2010; 194:668–674. [PubMed: 20173143]
21. Chang ST, Jeffrey RB, Patel BN, et al. Preoperative Multidetector CT Diagnosis of Extrapancreatic Perineural or Duodenal Invasion Is Associated with Reduced Postoperative Survival after

- Pancreaticoduodenectomy for Pancreatic Adenocarcinoma: Preliminary Experience and Implications for Patient Care. *Radiology*. 2016; 281:816–825. [PubMed: 27438167]
22. D’Onofrio M, Gallotti A, Mantovani W, et al. Perfusion CT can predict tumoral grading of pancreatic adenocarcinoma. *Eur J Radiol*. 2013; 82:227–233. [PubMed: 23127804]
 23. Prokesch RW, Chow LC, Beaulieu CF, et al. Isoattenuating pancreatic adenocarcinoma at multi-detector row CT: secondary signs. *Radiology*. 2002; 224:764–768. [PubMed: 12202711]
 24. Kauhanen SP, Komar G, Seppanen MP, et al. A prospective diagnostic accuracy study of 18F-fluorodeoxyglucose positron emission tomography/computed tomography, multidetector row computed tomography, and magnetic resonance imaging in primary diagnosis and staging of pancreatic cancer. *Ann Surg*. 2009; 250:957–963. [PubMed: 19687736]
 25. Bipat S, Phoa SS, van Delden OM, et al. Ultrasonography, computed tomography and magnetic resonance imaging for diagnosis and determining resectability of pancreatic adenocarcinoma: a meta-analysis. *J Comput Assist Tomogr*. 2005; 29:438–445. [PubMed: 16012297]
 26. Raman SP, Horton KM, Fishman EK. Multimodality imaging of pancreatic cancer-computed tomography, magnetic resonance imaging, and positron emission tomography. *Cancer J*. 2012; 18:511–522. [PubMed: 23187837]
 27. Adamek HE, Albert J, Breer H, et al. Pancreatic cancer detection with magnetic resonance cholangiopancreatography and endoscopic retrograde cholangiopancreatography: a prospective controlled study. *Lancet*. 2000; 356:190–193. [PubMed: 10963196]
 28. Vachiranubhap B, Kim YH, Balci NC, et al. Magnetic resonance imaging of adenocarcinoma of the pancreas. *Top Magn Reson Imaging*. 2009; 20:3–9. [PubMed: 19687720]
 29. Epelbaum R, Frenkel A, Haddad R, et al. Tumor aggressiveness and patient outcome in cancer of the pancreas assessed by dynamic 18F-FDG PET/CT. *J Nucl Med*. 2013; 54:12–18. [PubMed: 23166388]
 30. Lee JW, Kang CM, Choi HJ, et al. Prognostic value of metabolic tumor volume and total lesion glycolysis on preoperative 18F-FDG PET/CT in patients with pancreatic cancer. *Journal of Nuclear Medicine*. 2014; 55:898–904. [PubMed: 24711649]
 31. Gambhir SS, Czernin J, Schwimmer J, et al. A tabulated summary of the FDG PET literature. *J Nucl Med*. 2001; 42:1S–93S. [PubMed: 11483694]
 32. Choi M, Heilbrun LK, Venkatramanamoorthy R, et al. Using 18F-fluorodeoxyglucose positron emission tomography to monitor clinical outcomes in patients treated with neoadjuvant chemoradiotherapy for locally advanced pancreatic cancer. *Am J Clin Oncol*. 2010; 33:257–261. [PubMed: 19806035]
 33. Ghaneh P, Wong WL, Titman A, et al. PET-PANC: Multi-centre prospective diagnostic accuracy and clinical value trial of FDG PET/CT in the diagnosis and management of suspected pancreatic cancer. *J Clin Oncol*. 2016; 34(15 suppl) abstr 4008.
 34. Yokoyama Y, Nagino M, Hiromatsu T, et al. Intense PET signal in the degenerative necrosis superimposed on chronic pancreatitis. *Pancreas*. 2005; 31:192–194. [PubMed: 16025008]
 35. Vahrmeijer AL, Hutteman M, van der Vorst JR, et al. Image-guided cancer surgery using near-infrared fluorescence. *Nat Rev Clin Oncol*. 2013; 10:507–518. [PubMed: 23881033]
 36. Olubiyi OI, Ozdemir A, Incekara F, et al. Intraoperative Magnetic Resonance Imaging in Intracranial Glioma Resection: A Single-Center, Retrospective Blinded Volumetric Study. *World Neurosurg*. 2015; 84:528–536. [PubMed: 25937354]
 37. Nelson DW, Blanchard TH, Causey MW, et al. Examining the accuracy and clinical usefulness of intraoperative frozen section analysis in the management of pancreatic lesions. *Am J Surg*. 2013; 205:613–617. discussion 617. [PubMed: 23592172]
 38. Kooby DA, Lad NL, Squires MH 3rd, et al. Value of intraoperative neck margin analysis during Whipple for pancreatic adenocarcinoma: a multicenter analysis of 1399 patients. *Ann Surg*. 2014; 260:494–501. discussion 501–503. [PubMed: 25115425]
 39. Lad NL, Squires MH, Maithel SK, et al. Is it time to stop checking frozen section neck margins during pancreaticoduodenectomy? *Ann Surg Oncol*. 2013; 20:3626–3633. [PubMed: 23838908]
 40. Dillhoff M, Yates R, Wall K, et al. Intraoperative assessment of pancreatic neck margin at the time of pancreaticoduodenectomy increases likelihood of margin-negative resection in patients with pancreatic cancer. *J Gastrointest Surg*. 2009; 13:825–830. [PubMed: 19277793]

41. Harris PL, Rumley TO, Lineaweaver WC, et al. Pancreatic cancer: unreliability of frozen section in diagnosis. *South Med J*. 1985; 78:1053–1056. [PubMed: 4035430]
42. Witz M, Shkolnik Z, Dinbar A. Intraoperative pancreatic biopsy--a diagnostic dilemma. *J Surg Oncol*. 1989; 42:117–119. [PubMed: 2796345]
43. Kruskal JB, Kane RA. Intraoperative ultrasonography of the pancreas: techniques and clinical applications. *Surg Technol Int*. 1997; 6:49–57. [PubMed: 16160955]
44. Sun MR, Brennan DD, Kruskal JB, et al. Intraoperative ultrasonography of the pancreas. *Radiographics*. 2010; 30:1935–1953. [PubMed: 21057128]
45. Hata S, Imamura H, Aoki T, et al. Value of visual inspection, bimanual palpation, and intraoperative ultrasonography during hepatic resection for liver metastases of colorectal carcinoma. *World J Surg*. 2011; 35:2779–2787. [PubMed: 21959929]
46. Handgraaf HJ, Boonstra MC, Van Erkel AR, et al. Current and future intraoperative imaging strategies to increase radical resection rates in pancreatic cancer surgery. *Biomed Res Int*. 2014; 2014:890230. [PubMed: 25157372]
47. Bussom, S., Saif, MW. Methods and rationale for the early detection of pancreatic cancer. JOP; Highlights from the “2010 ASCO Gastrointestinal Cancers Symposium”; Orlando, FL, USA. January 22–24, 2010; 2010. p. 128-130.
48. Mondal SB, Gao S, Zhu N, et al. Real-time fluorescence image-guided oncologic surgery. *Adv Cancer Res*. 2014; 124:171–211. [PubMed: 25287689]
49. Conroy T, Desseigne F, Ychou M, et al. FOLFIRINOX versus gemcitabine for metastatic pancreatic cancer. *N Engl J Med*. 2011; 364:1817–1825. [PubMed: 21561347]
50. Ferrone CR, Marchegiani G, Hong TS, et al. Radiological and surgical implications of neoadjuvant treatment with FOLFIRINOX for locally advanced and borderline resectable pancreatic cancer. *Ann Surg*. 2015; 261:12–17. [PubMed: 25599322]
51. Wang YY, Cui QC. [Recent advances in gene change of pancreatic cancer]. [Article in Chinese]. *Zhongguo Yi Xue Ke Xue Yuan Xue Bao*. 2004; 26:79–82. [PubMed: 15052782]
52. Jones S, Zhang X, Parsons DW, et al. Core signaling pathways in human pancreatic cancers revealed by global genomic analyses. *Science*. 2008; 321:1801–1806. [PubMed: 18772397]
53. Harsha HC, Kandasamy K, Ranganathan P, et al. A compendium of potential biomarkers of pancreatic cancer. *PLoS Med*. 2009; 6:e1000046. [PubMed: 19360088]
54. van Oosten M, Crane LM, Bart J, et al. Selecting Potential Targetable Biomarkers for Imaging Purposes in Colorectal Cancer Using TArget Selection Criteria (TASC): A Novel Target Identification Tool. *Transl Oncol*. 2011; 4:71–82. [PubMed: 21461170]
55. James ML, Gambhir SS. A molecular imaging primer: modalities, imaging agents, and applications. *Physiol Rev*. 2012; 92:897–965. [PubMed: 22535898]
56. Argani P, Rosty C, Reiter RE, et al. Discovery of new markers of cancer through serial analysis of gene expression: prostate stem cell antigen is overexpressed in pancreatic adenocarcinoma. *Cancer Res*. 2001; 61:4320–4324. [PubMed: 11389052]
57. Iacobuzio-Donahue CA, Ashfaq R, Maitra A, et al. Highly expressed genes in pancreatic ductal adenocarcinomas: a comprehensive characterization and comparison of the transcription profiles obtained from three major technologies. *Cancer Res*. 2003; 63:8614–8622. [PubMed: 14695172]
58. Nichols LS, Ashfaq R, Iacobuzio-Donahue CA. Claudin 4 protein expression in primary and metastatic pancreatic cancer: support for use as a therapeutic target. *Am J Clin Pathol*. 2004; 121:226–230. [PubMed: 14983936]
59. Korner M, Hayes GM, Rehmann R, et al. Secretin receptors in normal and diseased human pancreas: marked reduction of receptor binding in ductal neoplasia. *Am J Pathol*. 2005; 167:959–968. [PubMed: 16192632]
60. Jensen RT, Wank SA, Rowley WH, et al. Interaction of CCK with pancreatic acinar cells. *Trends Pharmacol Sci*. 1989; 10:418–423. [PubMed: 2694538]
61. Reubi JC. In vitro evaluation of VIP/PACAP receptors in healthy and diseased human tissues. Clinical implications. *Ann N Y Acad Sci*. 2000; 921:1–25. [PubMed: 11193811]
62. Nock B, Nikolopoulou A, Chiotellis E, et al. [99mTc]Demobesin 1, a novel potent bombesin analogue for GRP receptor-targeted tumour imaging. *Eur J Nucl Med Mol Imaging*. 2003; 30:247–258. [PubMed: 12552343]

63. Yang L, Mao H, Cao Z, et al. Molecular imaging of pancreatic cancer in an animal model using targeted multifunctional nanoparticles. *Gastroenterology*. 2009; 136:1514–1525. [PubMed: 19208341]
64. Montet X, Weissleder R, Josephson L. Imaging pancreatic cancer with a peptide-nanoparticle conjugate targeted to normal pancreas. *Bioconjug Chem*. 2006; 17:905–911. [PubMed: 16848396]
65. Sofuni A, Iijima H, Moriyasu F, et al. Differential diagnosis of pancreatic tumors using ultrasound contrast imaging. *J Gastroenterol*. 2005; 40:518–525. [PubMed: 15942718]
66. Fan Z, Li Y, Yan K, et al. Application of contrast-enhanced ultrasound in the diagnosis of solid pancreatic lesions--a comparison of conventional ultrasound and contrast-enhanced CT. *Eur J Radiol*. 2013; 82:1385–1390. [PubMed: 23727375]
67. Kitano M, Kudo M, Yamao K, et al. Characterization of small solid tumors in the pancreas: the value of contrast-enhanced harmonic endoscopic ultrasonography. *Am J Gastroenterol*. 2012; 107:303–310. [PubMed: 22008892]
68. Pysz MA, Willmann JK. Targeted contrast-enhanced ultrasound: an emerging technology in abdominal and pelvic imaging. *Gastroenterology*. 2011; 140:785–790. [PubMed: 21255573]
69. Deshpande N, Needles A, Willmann JK. Molecular ultrasound imaging: current status and future directions. *Clin Radiol*. 2010; 65:567–581. [PubMed: 20541656]
70. Kircher MF, Willmann JK. Molecular body imaging: MR imaging, CT, and US. part I. principles. *Radiology*. 2012; 263:633–643. [PubMed: 22623690]
71. Kircher MF, Willmann JK. Molecular body imaging: MR imaging, CT, and US. Part II. Applications. *Radiology*. 2012; 264:349–368. [PubMed: 22821695]
72. Abou-Elkacem L, Bachawal SV, Willmann JK. Ultrasound molecular imaging: Moving toward clinical translation. *Eur J Radiol*. 2015; 84:1685–1693. [PubMed: 25851932]
73. Tranquart F, Arditì M, Bettinger T, et al. Ultrasound Contrast Agents For Ultrasound Molecular Imaging. *Z Gastroenterol*. 2014; 52:1268–1276. [PubMed: 25390214]
74. Bergers G, Benjamin LE. Tumorigenesis and the angiogenic switch. *Nat Rev Cancer*. 2003; 3:401–410. [PubMed: 12778130]
75. de Geus SW, Boogerd LS, Swijnenburg RJ, et al. Selecting Tumor-Specific Molecular Targets in Pancreatic Adenocarcinoma: Paving the Way for Image-Guided Pancreatic Surgery. *Mol Imaging Biol*. 2016; 18:807–819. [PubMed: 27130234]
76. Pysz MA, Machtaler SB, Seeley ES, et al. Vascular endothelial growth factor receptor type 2-targeted contrast-enhanced US of pancreatic cancer neovasculature in a genetically engineered mouse model: potential for earlier detection. *Radiology*. 2015; 274:790–799. [PubMed: 25322341]
77. Deshpande N, Ren Y, Foygel K, et al. Tumor angiogenic marker expression levels during tumor growth: longitudinal assessment with molecularly targeted microbubbles and US imaging. *Radiology*. 2011; 258:804–811. [PubMed: 21339349]
78. Willmann JK, Bonomo L, Carla Testa A, et al. Ultrasound Molecular Imaging With BR55 in Patients With Breast and Ovarian Lesions: First-in-Human Results. *J Clin Oncol*. 2017; 35:2133–2140. [PubMed: 28291391]
79. Foygel K, Wang H, Machtaler S, et al. Detection of pancreatic ductal adenocarcinoma in mice by ultrasound imaging of thymocyte differentiation antigen 1. *Gastroenterology*. 2013; 145:885–894. [PubMed: 23791701]
80. Pirollo KF, Dagata J, Wang P, et al. A tumor-targeted nanodelivery system to improve early MRI detection of cancer. *Mol Imaging*. 2006; 5:41–52. [PubMed: 16779969]
81. Yang L, Mao H, Wang YA, et al. Single chain epidermal growth factor receptor antibody conjugated nanoparticles for in vivo tumor targeting and imaging. *Small*. 2009; 5:235–243. [PubMed: 19089838]
82. Bausch D, Thomas S, Mino-Kenudson M, et al. Plectin-1 as a novel biomarker for pancreatic cancer. *Clin Cancer Res*. 2011; 17:302–309. [PubMed: 21098698]
83. Medarova Z, Pham W, Kim Y, et al. In vivo imaging of tumor response to therapy using a dual-modality imaging strategy. *Int J Cancer*. 2006; 118:2796–2802. [PubMed: 16385568]
84. Moore A, Medarova Z, Potthast A, et al. In vivo targeting of underglycosylated MUC-1 tumor antigen using a multimodal imaging probe. *Cancer Res*. 2004; 64:1821–1827. [PubMed: 14996745]

85. Dorn DC, Harnack U, Pecher G. Down-regulation of the human tumor antigen mucin by gemcitabine on the pancreatic cancer cell line capan-2. *Anticancer Res.* 2004; 24:821–825. [PubMed: 15161033]
86. Aung W, Jin ZH, Furukawa T, et al. Micro-positron emission tomography/contrast-enhanced computed tomography imaging of orthotopic pancreatic tumor-bearing mice using the alphavbeta(3) integrin tracer (6)(4)Cu-labeled cyclam-RAFT-c(-RGDfK-)(4). *Mol Imaging.* 2013; 12:376–387. [PubMed: 23981783]
87. Haglund C, Lindgren J, Roberts PJ, et al. Gastrointestinal cancer-associated antigen CA 19-9 in histological specimens of pancreatic tumours and pancreatitis. *Br J Cancer.* 1986; 53:189–195. [PubMed: 3513813]
88. Loy TS, Sharp SC, Andershock CJ, et al. Distribution of CA 19-9 in adenocarcinomas and transitional cell carcinomas. An immunohistochemical study of 527 cases. *Am J Clin Pathol.* 1993; 99:726–728. [PubMed: 8322708]
89. Houghton JL, Zeglis BM, Abdel-Atti D, et al. Site-specifically labeled CA19.9-targeted immunoconjugates for the PET, NIRF, and multimodal PET/NIRF imaging of pancreatic cancer. *Proc Natl Acad Sci U S A.* 2015; 112:15850–15855. [PubMed: 26668398]
90. Makovitzky J. The distribution and localization of the monoclonal antibody-defined antigen 19-9 (CA 19-9) in chronic pancreatitis and pancreatic carcinoma. An immunohistochemical study. *Virchows Arch B Cell Pathol Incl Mol Pathol.* 1986; 51:535–544. [PubMed: 2878526]
91. Hackel BJ, Kimura RH, Miao Z, et al. 18F-fluorobenzoate-labeled cystine knot peptides for PET imaging of integrin alphavbeta6. *J Nucl Med.* 2013; 54:1101–1105. [PubMed: 23670900]
92. Hausner SH, Abbey CK, Bold RJ, et al. Targeted in vivo imaging of integrin alphavbeta6 with an improved radiotracer and its relevance in a pancreatic tumor model. *Cancer Res.* 2009; 69:5843–5850. [PubMed: 19549907]
93. Gao D, Gao L, Zhang C, et al. A near-infrared phthalocyanine dye-labeled agent for integrin alphavbeta6-targeted theranostics of pancreatic cancer. *Biomaterials.* 2015; 53:229–238. [PubMed: 25890722]
94. Kimura RH, Teed R, Hackel BJ, et al. Pharmacokinetically stabilized cystine knot peptides that bind alpha-v-beta-6 integrin with single-digit nanomolar affinities for detection of pancreatic cancer. *Clin Cancer Res.* 2012; 18:839–849. [PubMed: 22173551]
95. Liu Z, Liu H, Ma T, et al. Integrin alphavbeta6-Targeted SPECT Imaging for Pancreatic Cancer Detection. *J Nucl Med.* 2014; 55:989–994. [PubMed: 24711651]
96. Zhu X, Li J, Hong Y, et al. 99mTc-labeled cystine knot peptide targeting integrin alphavbeta6 for tumor SPECT imaging. *Mol Pharm.* 2014; 11:1208–1217. [PubMed: 24524409]
97. van den Berg YW, Osanto S, Reitsma PH, et al. The relationship between tissue factor and cancer progression: insights from bench and bedside. *Blood.* 2012; 119:924–932. [PubMed: 22065595]
98. Nitori N, Ino Y, Nakanishi Y, et al. Prognostic significance of tissue factor in pancreatic ductal adenocarcinoma. *Clin Cancer Res.* 2005; 11:2531–2539. [PubMed: 15814630]
99. Hong H, Zhang Y, Nayak TR, et al. Immuno-PET of tissue factor in pancreatic cancer. *J Nucl Med.* 2012; 53:1748–1754. [PubMed: 22988057]
100. Chen R, Yi EC, Donohoe S, et al. Pancreatic cancer proteome: the proteins that underlie invasion, metastasis, and immunologic escape. *Gastroenterology.* 2005; 129:1187–1197. [PubMed: 16230073]
101. McCabe KE, Liu B, Marks JD, et al. An engineered cysteine-modified diabody for imaging activated leukocyte cell adhesion molecule (ALCAM)-positive tumors. *Mol Imaging Biol.* 2012; 14:336–347. [PubMed: 21630083]
102. Ryschich E, Huszty G, Knaebel HP, et al. Transferrin receptor is a marker of malignant phenotype in human pancreatic cancer and in neuroendocrine carcinoma of the pancreas. *Eur J Cancer.* 2004; 40:1418–1422. [PubMed: 15177502]
103. Sugyo A, Tsuji AB, Sudo H, et al. Preclinical evaluation of (8)(9)Zr-labeled human antitransferrin receptor monoclonal antibody as a PET probe using a pancreatic cancer mouse model. *Nucl Med Commun.* 2015; 36:286–294. [PubMed: 25460304]
104. de Boer E, Harlaar NJ, Taruttis A, et al. Optical innovations in surgery. *Br J Surg.* 2015; 102:e56–e72. [PubMed: 25627136]

105. van der Vorst JR, Schaafsma BE, Hutteman M, et al. Near-infrared fluorescence-guided resection of colorectal liver metastases. *Cancer*. 2013; 119:3411–3418. [PubMed: 23794086]
106. Troyan SL, Kianzad V, Gibbs-Strauss SL, et al. The FLARE intraoperative near-infrared fluorescence imaging system: a first-in-human clinical trial in breast cancer sentinel lymph node mapping. *Ann Surg Oncol*. 2009; 16:2943–2952. [PubMed: 19582506]
107. Mieog JS, Troyan SL, Hutteman M, et al. Toward optimization of imaging system and lymphatic tracer for near-infrared fluorescent sentinel lymph node mapping in breast cancer. *Ann Surg Oncol*. 2011; 18:2483–2491. [PubMed: 21360250]
108. van Dam GM, Themelis G, Crane LM, et al. Intraoperative tumor-specific fluorescence imaging in ovarian cancer by folate receptor-alpha targeting: first in-human results. *Nat Med*. 2011; 17:1315–1319. [PubMed: 21926976]
109. van der Vorst JR, Schaafsma BE, Verbeek FP, et al. Dose optimization for near-infrared fluorescence sentinel lymph node mapping in patients with melanoma. *Br J Dermatol*. 2013; 168:93–98. [PubMed: 23078649]
110. Crane LM, Themelis G, Arts HJ, et al. Intraoperative near-infrared fluorescence imaging for sentinel lymph node detection in vulvar cancer: first clinical results. *Gynecol Oncol*. 2011; 120:291–295. [PubMed: 21056907]
111. Hutteman M, van der Vorst JR, Gaarenstroom KN, et al. Optimization of near-infrared fluorescent sentinel lymph node mapping for vulvar cancer. *Am J Obstet Gynecol*. 2012; 206:89, e1–e5. [PubMed: 21963099]
112. van der Vorst JR, Hutteman M, Gaarenstroom KN, et al. Optimization of near-infrared fluorescent sentinel lymph node mapping in cervical cancer patients. *Int J Gynecol Cancer*. 2011; 21:1472–1478. [PubMed: 22027751]
113. Crane LM, Themelis G, Pleijhuis RG, et al. Intraoperative multispectral fluorescence imaging for the detection of the sentinel lymph node in cervical cancer: a novel concept. *Mol Imaging Biol*. 2011; 13:1043–1049. [PubMed: 20835767]
114. Zhang C, Kimura R, Abou-Elkacem L, et al. A Cystine Knot Peptide Targeting Integrin α v β 6 for Photoacoustic and Fluorescence Imaging of Tumors in Living Subjects. *J Nucl Med*. 2016; 57:1629–1634. [PubMed: 27230926]
115. Cruz-Monserrate Z, Abd-Elgaliel WR, Grote T, et al. Detection of pancreatic cancer tumours and precursor lesions by cathepsin E activity in mouse models. *Gut*. 2012; 61:1315–1322. [PubMed: 22068166]
116. Abd-Elgaliel WR, Cruz-Monserrate Z, Logsdon CD, et al. Molecular imaging of Cathepsin E-positive tumors in mice using a novel protease-activatable fluorescent probe. *Mol Biosyst*. 2011; 7:3207–3213. [PubMed: 21935563]
117. Weissleder R, Tung CH, Mahmood U, et al. In vivo imaging of tumors with protease-activated near-infrared fluorescent probes. *Nat Biotechnol*. 1999; 17:375–378. [PubMed: 10207887]
118. Hellebust A, Richards-Kortum R. Advances in molecular imaging: targeted optical contrast agents for cancer diagnostics. *Nanomedicine (Lond)*. 2012; 7:429–445. [PubMed: 22385200]
119. Whitley MJ, Cardona DM, Lazarides AL, et al. A mouse-human phase 1 co-clinical trial of a protease-activated fluorescent probe for imaging cancer. *Sci Transl Med*. 2016; 8:320ra4.
120. Zackrisson S, van de Ven SM, Gambhir SS. Light in and sound out: emerging translational strategies for photoacoustic imaging. *Cancer Res*. 2014; 74:979–1004. [PubMed: 24514041]
121. Wilson KE, Wang TY, Willmann JK. Acoustic and photoacoustic molecular imaging of cancer. *J Nucl Med*. 2013; 54:1851–1854. [PubMed: 24187042]
122. Valluru KS, Wilson KE, Willmann JK. Photoacoustic Imaging in Oncology: Translational Preclinical and Early Clinical Experience. *Radiology*. 2016; 280:332–349. [PubMed: 27429141]
123. Valluru KS, Willmann JK. Clinical photoacoustic imaging of cancer. *Ultrasonography*. 2016; 35:267–280. [PubMed: 27669961]
124. Homan KA, Souza M, Truby R, et al. Silver nanoplate contrast agents for in vivo molecular photoacoustic imaging. *ACS Nano*. 2012; 6:641–650. [PubMed: 22188516]
125. Kim G, Huang SW, Day KC, et al. Indocyanine-green-embedded PEBBLEs as a contrast agent for photoacoustic imaging. *J Biomed Opt*. 2007; 12:044020. [PubMed: 17867824]

126. Brakmane G, Madani SY, Seifalian A. Cancer antibody enhanced real time imaging cell probes--a novel theranostic tool using polymer linked carbon nanotubes and quantum dots. *Anticancer Agents Med Chem.* 2013; 13:821–832. [PubMed: 23537047]
127. De la Zerda A, Zavaleta C, Keren S, et al. Carbon nanotubes as photoacoustic molecular imaging agents in living mice. *Nat Nanotechnol.* 2008; 3:557–562. [PubMed: 18772918]
128. Erogbogbo F, Liu X, May JL, et al. Plasmonic gold and luminescent silicon nanoplatfoms for multimode imaging of cancer cells. *Integr Biol (Camb).* 2013; 5:144–150. [PubMed: 23014624]
129. Shashkov EV, Everts M, Galanzha EI, et al. Quantum dots as multimodal photoacoustic and photothermal contrast agents. *Nano Lett.* 2008; 8:3953–3958. [PubMed: 18834183]
130. Zaman MB, Baral TN, Jakubek ZJ, et al. Single-domain antibody bioconjugated near-IR quantum dots for targeted cellular imaging of pancreatic cancer. *J Nanosci Nanotechnol.* 2011; 11:3757–3763. [PubMed: 21780366]
131. Jain RK. Delivery of molecular medicine to solid tumors: lessons from in vivo imaging of gene expression and function. *J Control Release.* 2001; 74:7–25. [PubMed: 11489479]
132. Wilson KE, Bachawal SV, Abou-Elkacem L, et al. Spectroscopic Photoacoustic Molecular Imaging of Breast Cancer using a B7-H3-targeted ICG contrast agent. *Theranostics.* 2017; 7:1463–1476. [PubMed: 28529630]
133. Levi J, Sathirachinda A, Gambhir SS. A high-affinity, high-stability photoacoustic agent for imaging gastrin-releasing peptide receptor in prostate cancer. *Clin Cancer Res.* 2014; 20:3721–3729. [PubMed: 24850845]
134. Levi J, Kothapalli SR, Bohndiek S, et al. Molecular photoacoustic imaging of follicular thyroid carcinoma. *Clin Cancer Res.* 2013; 19:1494–1502. [PubMed: 23349314]
135. Li J, Liu J, Wei CW, et al. Emerging applications of conjugated polymers in molecular imaging. *Phys Chem Chem Phys.* 2013; 15:17006–17015. [PubMed: 23860904]
136. Balasundaram G, Ho CJ, Li K, et al. Molecular photoacoustic imaging of breast cancer using an actively targeted conjugated polymer. *Int J Nanomedicine.* 2015; 10:387–397. [PubMed: 25609951]
137. Levi J, Kothapalli SR, Ma TJ, et al. Design, synthesis, and imaging of an activatable photoacoustic probe. *J Am Chem Soc.* 2010; 132:11264–11269. [PubMed: 20698693]
138. Zavaleta CL, Kircher MF, Gambhir SS. Raman's "effect" on molecular imaging. *J Nucl Med.* 2011; 52:1839–1844. [PubMed: 21868625]
139. Jokerst JV, Pohling C, Gambhir SS. Molecular imaging with surface-enhanced Raman spectroscopy nanoparticle reporters. *MRS Bull.* 2013:38.
140. Jeanmaire DL, Van Duyne RP. Surface Raman Spectroelectrochemistry Part I. Heterocyclic, Aromatic, and Aliphatic Amines Adsorbed on the Anodized Silver Electrode. *J Electroanal Chem.* 1977; 84:1–20.
141. Fleischmann M, Hendra PJ, McQuillan AJ. Raman spectra of pyridine adsorbed at a silver electrode. *Chemical Physics Letters.* 1974; 26:163–166.
142. Zavaleta CL, Garai E, Liu JT, et al. A Raman-based endoscopic strategy for multiplexed molecular imaging. *Proc Natl Acad Sci U S A.* 2013; 110:E2288–E2297. [PubMed: 23703909]
143. Zavaleta CL, Hartman KB, Miao Z, et al. Preclinical evaluation of Raman nanoparticle biodistribution for their potential use in clinical endoscopy imaging. *Small.* 2011; 7:2232–2240. [PubMed: 21608124]
144. Garai E, Sensarn S, Zavaleta CL, et al. A real-time clinical endoscopic system for intraluminal, multiplexed imaging of surface-enhanced Raman scattering nanoparticles. *PLoS One.* 2015; 10:e0123185. [PubMed: 25923788]
145. Jermyn M, Mok K, Mercier J, et al. Intraoperative brain cancer detection with Raman spectroscopy in humans. *Sci Transl Med.* 2015; 7:274ra19.
146. Kircher MF, de la Zerda A, Jokerst JV, et al. A brain tumor molecular imaging strategy using a new triple-modality MRI-photoacoustic-Raman nanoparticle. *Nat Med.* 2012; 18:829–834. [PubMed: 22504484]
147. Stone N, Matousek P. Advanced transmission Raman spectroscopy: a promising tool for breast disease diagnosis. *Cancer Res.* 2008; 68:4424–4430. [PubMed: 18519705]

148. Fenn MB, Xanthopoulos P, Pyrgiotakis G, et al. Raman Spectroscopy for Clinical Oncology. *Advances in Optical Technologies*. 2011; 2011:20.
149. Tummers WS, Warram JM, Tipirneni KE, et al. Regulatory Aspects of Optical Methods and Exogenous Targets for Cancer Detection. *Cancer Res*. 2017; 77:2197–2206. [PubMed: 28428283]
150. Sipos B, Hahn D, Carceller A, et al. Immunohistochemical screening for beta6-integrin subunit expression in adenocarcinomas using a novel monoclonal antibody reveals strong up-regulation in pancreatic ductal adenocarcinomas in vivo and in vitro. *Histopathology*. 2004; 45:226–236. [PubMed: 15330800]
151. Girgis MD, Kenanova V, Olafsen T, et al. Anti-CA 19-9 diabody as a PET imaging probe for pancreas cancer. *J Surg Res*. 2011; 170:169–178. [PubMed: 21601881]
152. Azuma T, Yamada M, Murakita H, et al. Cathepsin E expressed in pancreatic cancer. *Adv Exp Med Biol*. 1995; 362:363–366. [PubMed: 8540344]
153. Michl P, Buchholz M, Rolke M, et al. Claudin-4: a new target for pancreatic cancer treatment using *Clostridium perfringens* enterotoxin. *Gastroenterology*. 2001; 121:678–684. [PubMed: 11522752]
154. Angelescu R, Burada F, Angelescu C, et al. Expression of vascular endothelial growth factor and epidermal growth factor receptor in pancreatic ductal adenocarcinomas, neuroendocrine tumours and chronic pancreatitis. *Endosc Ultrasound*. 2013; 2:86–91. [PubMed: 24949370]
155. Zhou L, Yu L, Ding G, et al. Overexpressions of DLL4 and CD105 are Associated with Poor Prognosis of Patients with Pancreatic Ductal Adenocarcinoma. *Pathol Oncol Res*. 2015; 21:1141–1147. [PubMed: 25986715]
156. Argani P, Iacobuzio-Donahue C, Ryu B, et al. Mesothelin is overexpressed in the vast majority of ductal adenocarcinomas of the pancreas: identification of a new pancreatic cancer marker by serial analysis of gene expression (SAGE). *Clin Cancer Res*. 2001; 7:3862–3868. [PubMed: 11751476]
157. Hassan R, Laszik ZG, Lerner M, et al. Mesothelin is overexpressed in pancreaticobiliary adenocarcinomas but not in normal pancreas and chronic pancreatitis. *Am J Clin Pathol*. 2005; 124:838–845. [PubMed: 16416732]
158. Matsuyama M, Kondo F, Ishihara T, et al. Evaluation of pancreatic intraepithelial neoplasia and mucin expression in normal pancreata. *J Hepatobiliary Pancreat Sci*. 2012; 19:242–248. [PubMed: 21644061]
159. Andrianifahanana M, Moniaux N, Schmied BM, et al. Mucin (MUC) gene expression in human pancreatic adenocarcinoma and chronic pancreatitis: a potential role of MUC4 as a tumor marker of diagnostic significance. *Clin Cancer Res*. 2001; 7:4033–4040. [PubMed: 11751498]
160. Moniaux N, Chakraborty S, Yalniz M, et al. Early diagnosis of pancreatic cancer: neutrophil gelatinase-associated lipocalin as a marker of pancreatic intraepithelial neoplasia. *Br J Cancer*. 2008; 98:1540–1547. [PubMed: 18392050]
161. Hogendorf P, Durczynski A, Skulimowski A, et al. Neutrophil Gelatinase-Associated Lipocalin (NGAL) concentration in urine is superior to CA 19-9 and Ca 125 in differentiation of pancreatic mass: Preliminary report. *Cancer Biomark*. 2016; 16:537–543. [PubMed: 27002756]
162. Wente MN, Jain A, Kono E, et al. Prostate stem cell antigen is a putative target for immunotherapy in pancreatic cancer. *Pancreas*. 2005; 31:119–125. [PubMed: 16024997]
163. Kakkar AK, Lemoine NR, Scully MF, et al. Tissue factor expression correlates with histological grade in human pancreatic cancer. *Br J Surg*. 1995; 82:1101–1104. [PubMed: 7648165]
164. Jeong SM, Hwang S, Seong RH. Transferrin receptor regulates pancreatic cancer growth by modulating mitochondrial respiration and ROS generation. *Biochem Biophys Res Commun*. 2016; 471:373–379. [PubMed: 26869514]
165. Zhu J, Thakolwiboon S, Liu X, et al. Overexpression of CD90 (Thy-1) in pancreatic adenocarcinoma present in the tumor microenvironment. *PLoS One*. 2014; 9:e115507. [PubMed: 25536077]
166. Cantero D, Friess H, Deflorin J, et al. Enhanced expression of urokinase plasminogen activator and its receptor in pancreatic carcinoma. *Br J Cancer*. 1997; 75:388–395. [PubMed: 9020484]

167. Boonstra MC, Verspaget HW, Ganesh S, et al. Clinical applications of the urokinase receptor (uPAR) for cancer patients. *Curr Pharm Des.* 2011; 17:1890–910. [PubMed: 21711239]
168. Pochon S, Tardy I, Bussat P, et al. BR55: a lipopeptide-based VEGFR2-targeted ultrasound contrast agent for molecular imaging of angiogenesis. *Invest Radiol.* 2010; 45:89–95. [PubMed: 20027118]
169. Hicklin DJ, Ellis LM. Role of the vascular endothelial growth factor pathway in tumor growth and angiogenesis. *J Clin Oncol.* 2005; 23:1011–1027. [PubMed: 15585754]

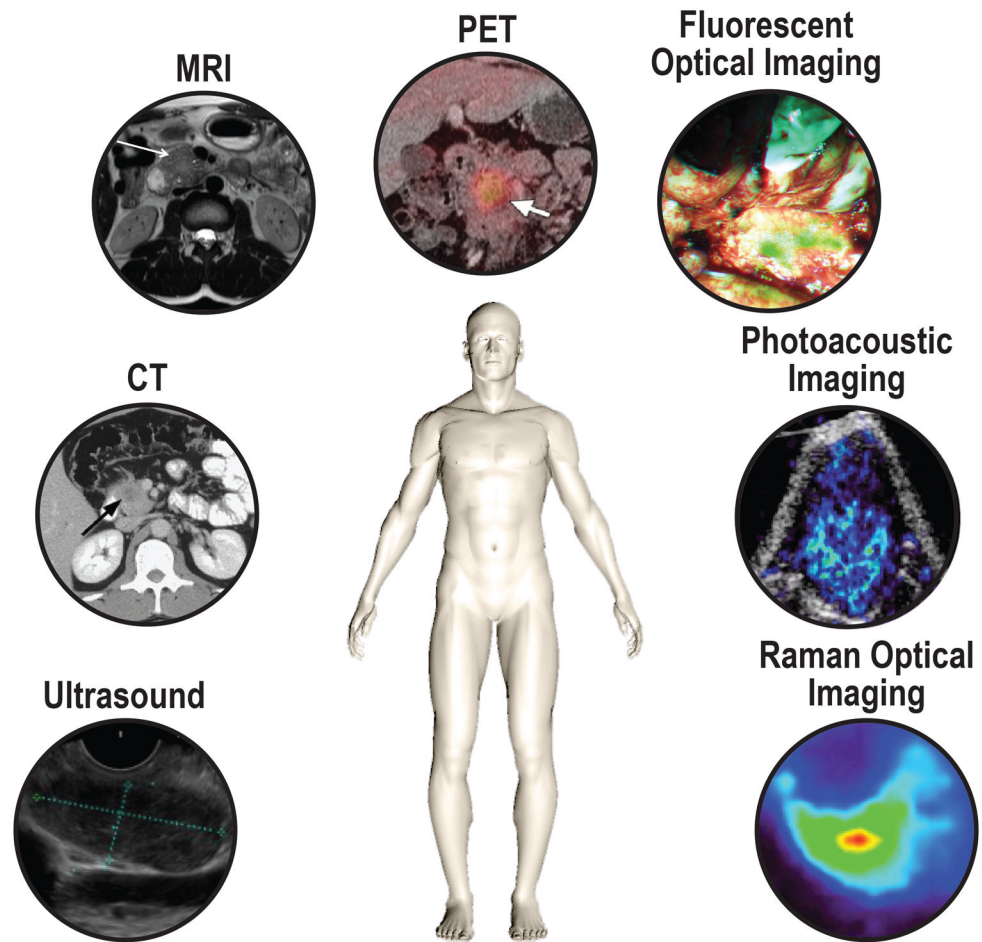


FIGURE 1. Schematic illustration of the key imaging modalities used for the diagnostics and potential intraoperative modalities for pancreatic cancer. Ultrasound, (endoscopic) ultrasound; CT, computed tomography; MRI, magnetic resonance imaging; PET, positron emission tomography. Representative images are shown of pancreatic cancer with the displayed modalities, expect for photoacoustic and raman optical imaging.

Intra-operative contrast-enhanced ultrasound

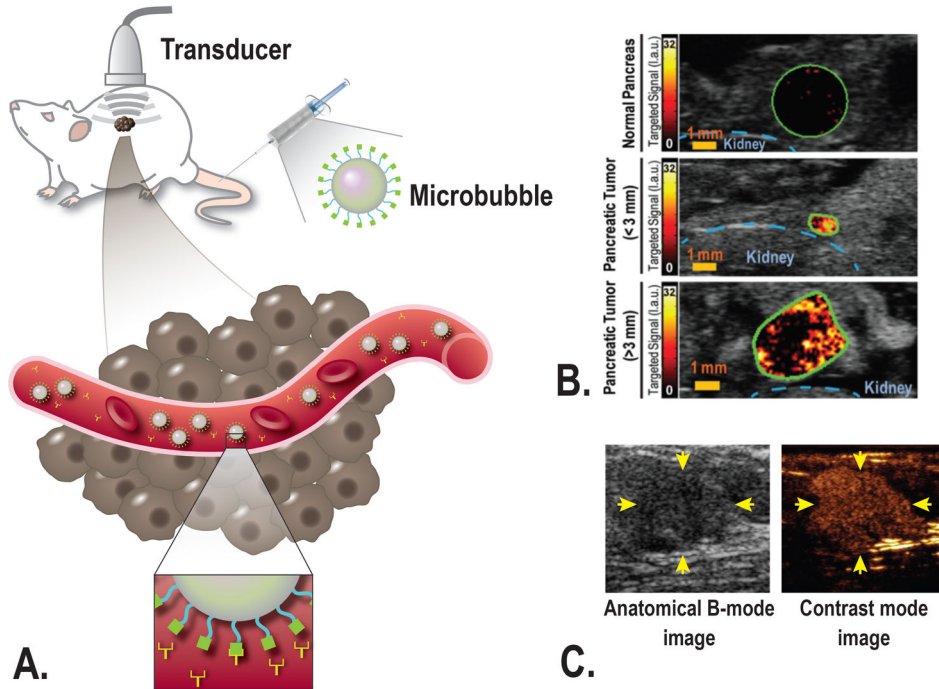
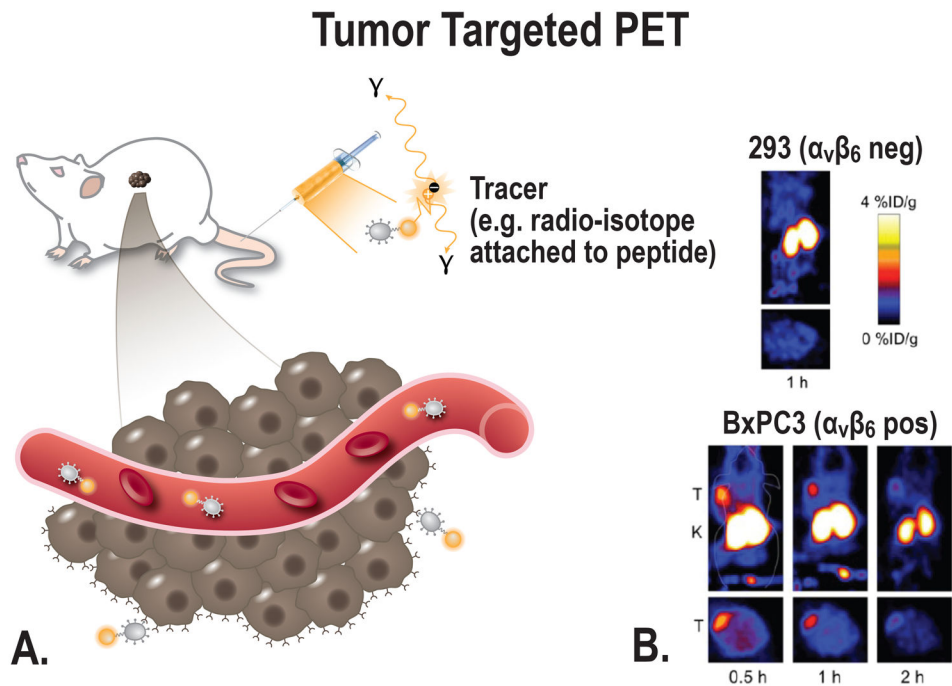
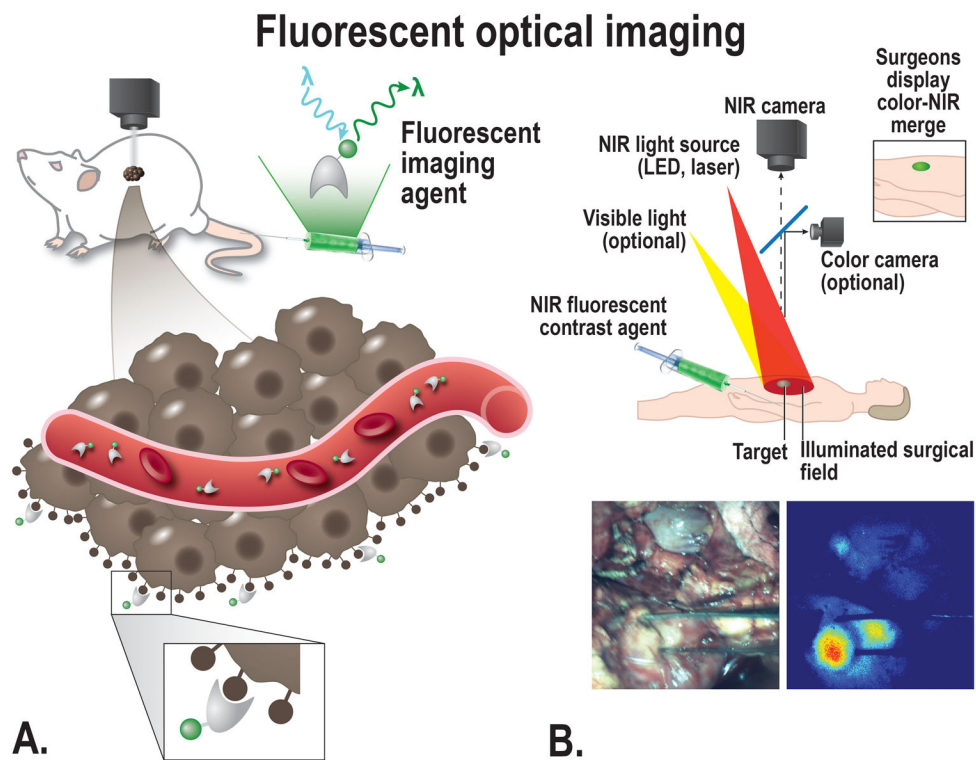


FIGURE 2.

A, Schematic overview of the principle of ultrasound molecular imaging. A molecularly-targeted contrast agent (microbubble) is administered intravenously into the subject (in this case a mouse). Sound waves are transmitted into the subject by the transducer, the sound wave reflections are recorded and converted into images. Because of the size of microbubbles of several micrometers, the contrast agent remains intravascular and attaches to the target of choice (for example VEGFR2). Examples of in vivo molecular ultrasound images with microbubbles in (B) transgenic mouse model of PDAC, showing a strong signal when targeting VEGFR2 in focus of PDAC compared to normal pancreatic tissue, even in small PDAC lesions [From Pysz et al, 2015⁷⁶], and (C) in human with breast cancer using microbubbles targeting kinase insert domain receptor (MB_{KDR}). Left panel: the anatomical image for reference, right panel: MB_{KDR} accumulation in breast cancer lesion [Willmann et al, 2017⁷⁸]

**FIGURE 3.**

A, Schematic overview of the principle of tumor-targeted PET imaging, a suitable tracer will be administered into the subject (in this case a mouse). Depending on the size of the tracer, the tracer can target the cancer at multiple locations; e.g. intravascular, receptors on the cell membrane, or intracellular. B, Small-animal PET imaging. BxPC-3 (integrin $\alpha_v\beta_6$ pos) and 293 (integrin $\alpha_v\beta_6$ negative) cells were xenografted in nude mice. PET images were acquired in tumor-bearing mice using a $\alpha_v\beta_6$ -targeted cysteine knot (^{18}F -fluorobenzoate- R_01) [From Hackel et al, 2013⁹¹].

**FIGURE 4.**

A, Schematic overview of the principle of fluorescent imaging, a suitable targeted imaging agent with a fluorescent dye will be administered into the subject (in this case a mouse). The agent is visualized using a fluorescence imaging system, with an adequate excitation laser and camera able to detect the emitted light. The targeted agents migrate to the cellular targets to visualize the tumor in a target-specific manner, the imaging agent can target the cancer at multiple locations depending on the size; e.g. intravascular, receptors on the cell membrane, or intracellular. B, Top: schematic overview showing the principle of fluorescent imaging. Bottom: Intraoperative image showing the use of tumor-targeted fluorescent guided imaging during pancreatic cancer surgery.

Photoacoustic imaging

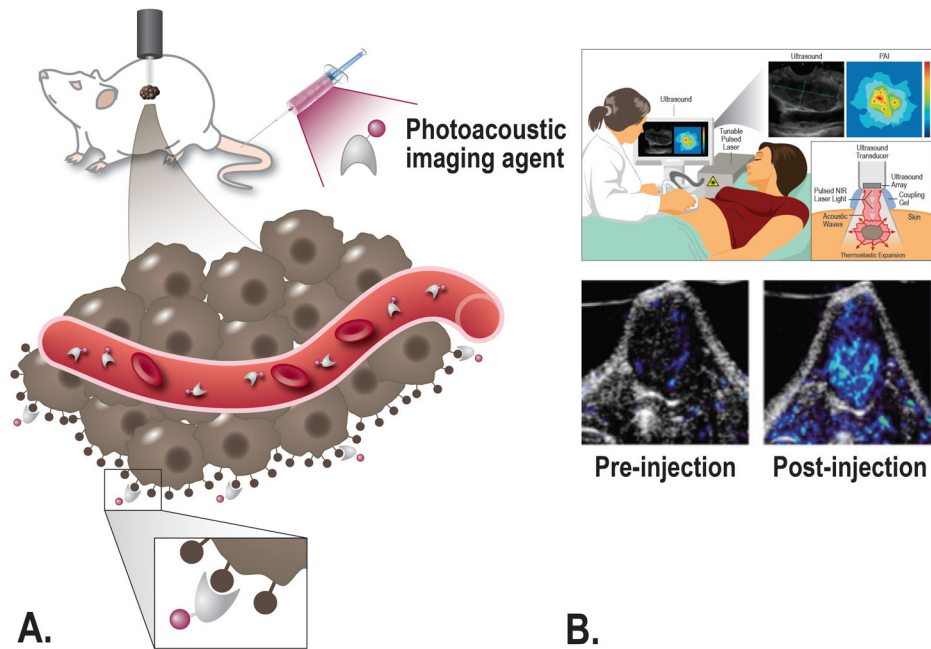


FIGURE 5. A, Schematic overview of photoacoustic imaging principle; after injection of a tumor-targeting agent the imaging agent will target tumor cells and produces an enhanced photoacoustic signal, after excitation with a laser. The agent can target the cancer at multiple locations depending on the size; e.g. intravascular, receptors on the cell membrane, or intracellular. B, Top: Schematic overview showing the principle of photoacoustic imaging; the thermo-elastic expansion caused by heating of the tissue due to the laser will lead to acoustic waves that can be converted into both ultrasound and molecular images. Bottom: Tumor-targeted photoacoustic imaging. Mice bearing FTC133 tumors were photoacoustically imaged using 680 and 750 nm light before and after the injection of a MMP-targeting probe [From Levi et al, 2013¹³⁴].

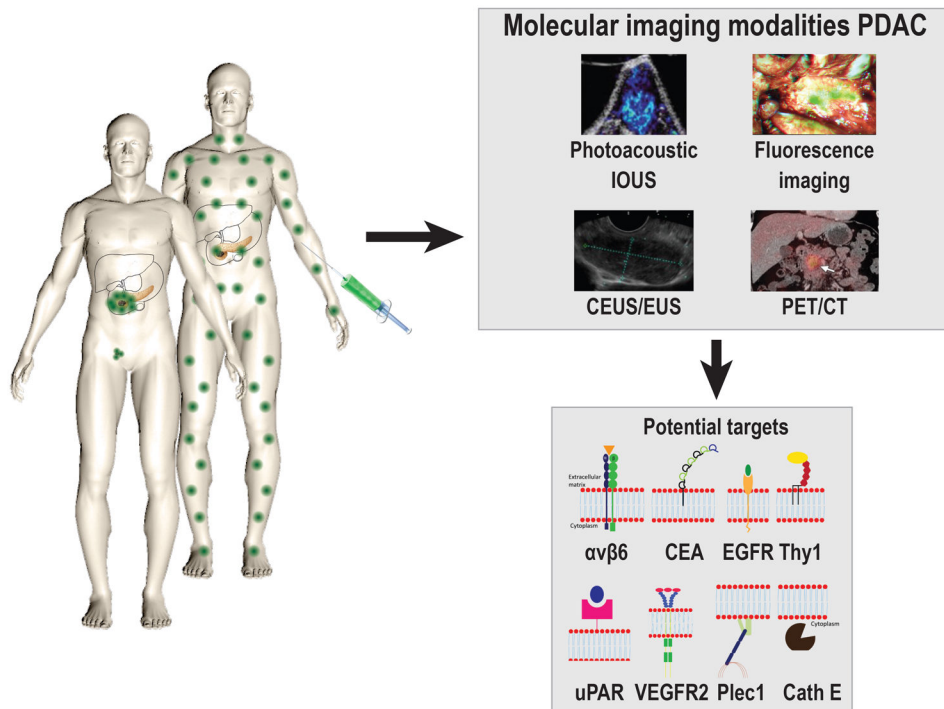


FIGURE 6. A schematic overview of the principle of tumor-targeted imaging in pancreatic cancer, showing the most promising imaging modalities for early diagnosis and improved surgical treatment, and most promising targets for this purpose. $\alpha v \beta 6$; Integrin $\alpha v \beta 6$, CEA; Carcinoembryonic Antigen, EGFR; Epidermal growth factor receptor, Thy1; Thy-1 cell surface antigen, uPAR; Urokinase receptor, VEGFR2; Vascular endothelial growth factor receptor 2, Plec1; Plectin 1, Cath E; Cathepsin E.

TABLE 1

Available Molecular Imaging Ligands With an Example, and the Main Advantages and Disadvantages

Type	Small Molecule	Peptide	Aptamer	Monoclonal Antibody	Protein Fragment (Diabody)	Nanoparticle	Microbubble
Size	<0.5 kDa	0.5–2 kDa	5–15 kDa	150 kDa	55 kDa	10–100 nm	1–4 μ m
Example	^{18}F -FDG	Cyclic RGD peptide	^{99}Tc -TTA-1	Cetuximab-IRDye800	^{18}F FB-T84.66	EGFR antibody-gold nanoparticle	VEGFR2-targeted microbubble
Advantage	Easy escape vasculature.	Easily modified. Superior selectivity.	Inexpensive production. High diversity.	High affinity and specificity.	Superior tumor penetration. High tumor- to blood ratio.	Effective delivery of signaling and therapeutic payload.	Good safety, wide availability of contrast mode ultrasound scanner
Drawback	Costly development. Limited size for the signaling component.	Rapid degradation.	Low in vivo stability. Poor membrane passage.	Slow clearance. Restricted in passing biological barriers.	Accumulation in kidneys.	Difficult extravasation due to size.	Imaging limited to molecular targeted differentially expressed on tumor vasculature

TABLE 2

Summary of Potential Targets Molecular Imaging Purposes for PDAC With Main Advantages and Disadvantages

Target	Type	Localization	Main Advantage	Main Disadvantage	References
ALCAM (CD166)	Glycoprotein in immunoglobulin family	Cell membrane	Expression in PDAC 2.5x higher compared to normal pancreatic tissue.	Expression on activated immune cells and the expression of ALCAM in pancreatitis is unknown.	100,101
$\alpha_5\beta_1$	Integrin	Cell membrane	Diffuse, strong expression in PDAC.	Mild expression on normal ductal tissue.	75,150
CA 19-9	Glycosylation product presented on cell surface proteins	Cell membrane	Expressed in up to 90% of all pancreatic cancers.	Expression on pancreatitis and normal ductal tissue.	87,88,90,151
Cath E	Proteolytic enzyme	Intracellular	Ideal for imaging purposes due to potential use of activatable probes and differentiation between PDAC, normal pancreatic tissue, and pancreatitis.	Intracellular location of target makes internalization of probe required.	53,115,152
Claudin 4	Integral membrane protein	Tight junctions	Upregulation in metastasis and expression in PanIN 3.	Ability to discriminate between PDAC and pancreatitis is unknown. Overexpression in PanIN 1 and 2.	58,153
EGFR	Receptor tyrosine kinase	Cell membrane	EGFR-mediated cellular internalization of targeted particles.	EGFR is expressed in pancreatitis and on duodenal tissue, which could potentially interfere with the surgical field.	75,81,154
Endoglin (CD105)	Type 1 membrane glycoprotein	Cell membrane	Expression levels vary throughout tumor growth, and overexpression is related to poor prognosis.	Expression is restricted to vascular endothelial cells undergoing active angiogenesis. Expression in pancreatitis is unknown.	77,155
Mesothelin	GPI-anchored glycoprotein	Cell membrane	Expressed in PDAC and not in normal pancreatic tissue or in pancreatitis.	Mesothelin is released into the bloodstream what could reduce the signal at tumor site.	156,157
Mucin-1	O-glycosylated proteins	Cell membrane	Expression on apical surface in normal tissue. Expression is correlated with more aggressive biological behavior.	Possible downregulation of expression after neoadjuvant therapy. Present in the RNA of pancreatitis patients.	85,158,159
NGAL	Secreted protein	Extracellular	Potential biomarker for early detection, can also differentiate between PDAC and pancreatitis in urine and bile.	Not bound on tumor cell membrane, which could complicate imaging specificity.	160,161
PCSA	GPI-anchored glycoprotein	Cell membrane	Upregulation in PDAC compared to pancreatitis and normal pancreatic tissue.	Overexpressed in only 60% of pancreatic cancers.	56,162
Plectin-1	Protein for linkage in cytoskeleton	Cytoplasm	Overexpressed in PDAC compared to normal pancreatic tissue and pancreatitis. Also expressed in PanIN 3 and is therefore a potential marker for early detection.	Target is expressed in the cytoplasm as opposed to on the cell membrane.	82
TF	Glycoprotein	Cell membrane	TF is used in staging and is correlated with incidence of metastases and with overall survival.	The expression of TF in pancreatitis in humans is unknown.	98,163
TTR	Glycoprotein	Cell membrane	Upregulation is induced by hypoxia, a known feature of PDAC.	Receptors are highly expressed in the liver. Expression of TTR in pancreatitis is unknown.	102,103,164
Thy1	GPI-anchored glycoprotein	Cell membrane	Marker for cancer-associated fibroblasts; also expressed on tumor vasculature but not in pancreatitis.	Thy1 is present on stromal cells, which is also upregulated in pancreatitis.	79,165

Author Manuscript

Author Manuscript

Author Manuscript

Author Manuscript

Target	Type	Localization	Main Advantage	Main Disadvantage	References
uPAR	GPI-anchored glycoprotein	Cell membrane	Expression on both tumor cells and stromal cells in the tumor microenvironment.	High uPAR staining in negative lymph nodes due to staining of tumor microenvironment.	75,166,167
VEGFR2	Receptor tyrosine kinase	Cell membrane	Upregulated in 72% of all PDAC cases.	Restricted to vascular endothelium. VEGFR2 expression is increased in pancreatitis.	75,154,168,169